ATP serves as a nucleotide switch coupling the genome maturation and packaging motor complexes of a virus assembly machine

Qin Yang and Carlos E. Catalano [ID]*

Skaggs School of Pharmacy and Pharmaceutical Sciences, Department of Pharmaceutical Chemistry, University of Colorado Anschutz Medical Campus, Aurora, CO 80045, USA

ABSTRACT

The assembly of double-stranded DNA viruses, from phages to herpesviruses, is strongly conserved. Terminase enzymes processively excise and package monomeric genomes from a concatemeric DNA substrate. The enzymes cycle between a stable maturation complex that introduces site-specific nicks into the duplex and a dynamic motor complex that rapidly translocates DNA into a procapsid shell, fueled by ATP hydrolysis. These tightly coupled reactions are catalyzed by terminase assembled into two functionally distinct nucleoprotein complexes; the maturation complex and the packaging motor complex, respectively. We describe the effects of nucleotides on the assembly of a catalytically competent maturation complex on viral DNA, their effect on maturation complex stability and their requirement for the transition to active packaging motor complex. ATP plays a major role in regulating all of these activities and may serve as a 'nucleotide switch' that mediates transitions between the two complexes during processive genome packaging. These biological processes are recapitulated in all of the dsDNA viruses that package monomeric genomes from concatemeric DNA substrates and the nucleotide switch mechanism may have broad biological implications with respect to virus assembly mechanisms.

INTRODUCTION

Viruses are obligate intracellular parasites whose developmental pathways are initiated upon insertion of their genetic material into the host cell. Subsequently, viral genomes and structural proteins are synthesized and the infectious particle is assembled utilizing a variety of viral and host-encoded biomolecules (1,2). The assembly pathways represent an ordered process that is generally conserved within broad classes, such as the large double-stranded DNA (dsDNA) viruses; these include the *Caudoviridae* (tailed bacteriophages), the *adenoviridae* and the *herpesviridae* (3–6).

The dsDNA viruses are composed of a genome tightly packaged into an icosahedral shell that is composed of hundreds of copies of a major capsid protein and twelve copies of a portal protein assembled into a ring-like structure at a unique vertex in the icosahedron (the portal vertex) (3,7,8); the portal provides a conduit for DNA egress from the shell during infection. Upon insertion into the cell, the viral genome is typically replicated via a rolling circle mechanism to afford linear concatemers of the viral genome linked head-to-tail (immature DNA) (9,10). Expression of late viral genes produces structural proteins that self-assemble into procapsid shells and a virus-encoded terminase enzyme that serves two essential functions; (i) nucleolytic excision of individual (mature) genomes from the concatemer (genome maturation reaction) and (ii) concomitant translocation of viral DNA into a preassembled procapsid shell (DNA packaging reaction) (7–13).

Terminase enzymes are heterooligomers composed of a large catalytic TerL subunit responsible for maturation and packaging activities and a small TerS subunit that is required for specific recognition of viral DNA. Both subunits are required to site-specifically assemble the maturation complex and they are both essential for virus development *in vivo* (3,8,11). Our lab studies the terminase enzyme from bacteriophage λ as a model system for dsDNA virus assembly. Phage λ assembly has been fully reconstituted *in vitro* and an infectious virus can be assembled using purified proteins and commercially available λ DNA (14); this allows interrogation of each step along the assembly pathway. The enzymology, biochemistry and biophysical features of λ terminase have been well described (14–22) and provides an ideal system with which to reveal mechanistic features of genome packaging in the dsDNA viruses (23).

*To whom correspondence should be addressed. Tel: +1 303 724 0011; Email: carlos.catalano@cuanschutz.edu

Phage λ genome maturation

λ terminase is composed of one TerL subunit and two TerS subunits in a stable heterotrimeric protomer complex (TerL$_1$•TerS$_2$, Figure 1A); however, the protomer is devoid of catalytic activity (16,24,25). At physiological concentrations, four protomers and the *Escherichia coli* Integration Host Factor (**IHF**) cooperatively assemble at the cohesive end sequence (*cos*) in concatemeric viral DNA, which represents the junction between two genomes in the concatemer and serves as the packaging initiation site (26). Assembly of this maturation complex, mediated by TerS interactions with repeating R-elements within the *cosB* subsite, activates an endonuclease activity that resides in a C-terminal domain of TerL and which introduces symmetric nicks into the *cosN* subsite (Figure 1B) (12). Release of the upstream D_R fragment affords the post-cleavage maturation complex composed of terminase tightly bound to the downstream D_L end of the first λ genome to be packaged. Both the pre-cleavage and post-cleavage maturation complexes are extremely stable ($T_{1/2}$ = 12 and 8 h, respectively), which ensures that the 12 base single-stranded end generated in the maturation reaction is sequestered from damaging exonucleases within the cell (27).

Phage λ genome packaging

The maturation complex next binds to the portal vertex of a pre-assembled procapsid shell to afford the packaging motor complex. This triggers a transition from the stable, site-specifically bound maturation complex to a dynamic, translocating motor complex (Figure 1B). We refer to this transition as *cos*-clearance and number of events must occur for the transition to packaging (23); (i) the endonuclease activity of TerL must be down-regulated, (ii) specific *cos*-binding interactions of must be broken, (iii) IHF specifically bound at *cosB* must be ejected from the complex and (iv) the packaging ATPase activity of TerL must be activated to power duplex translocation into the procapsid shell.

The activated packaging motor translocates DNA into the procapsid shell, fueled by ATP hydrolysis. Upon packaging ∼30% genome length (15 kb), the procapsid undergoes an expansion transition to afford a larger, thinner and more angularized structure known as the capsid (28–31). The λ decoration protein adds to the shell surface to stabilize the structure and the terminase motor continues to package the viral genome, ultimately to liquid crystalline density. Upon encountering the downstream *cos* site (the end of the genome), terminase again binds specifically to *cos*, halting motor translocation and re-generating a stable maturation complex (*cos*-capture). This requires down-regulation of packaging ATPase activity and re-activation the endonuclease activity of TerL which introduces symmetric nicks into the *cosN* subsite. Finishing proteins displace the terminase-DNA concatemer complex (shortened by one genome) to afford a nucleocapsid containing a single mature genome with cohesive D_L and D_R ends. The ejected terminase–concatemer complex binds to a second procapsid to initiate the next round of processive genome packaging (Figure 1B).

The fundamental features of processive genome packaging from a concatemeric DNA substrate, outlined in Figure 1B, are strongly conserved from phages to herpesviruses (1–3). This requires that the terminase enzymes processively alternate between a stable maturation complex that is tightly and specifically bound at inter-genomic assembly sites and a dynamic motor complex that rapidly translocates DNA in a non-specific manner. These tightly coupled reactions are catalyzed by terminase assembled into two functionally distinct nucleoprotein complexes; the maturation complex and the packaging motor complex, respectively. The factors that regulate the assembly of the complexes and the transitions between them has remained largely unexplored, primarily because sufficiently defined experimental systems have not been available. Here we describe the effects of nucleotides on the assembly of the λ maturation complex at *cos*, their role in activating the endonuclease activity of the enzyme, their effect on maturation complex stability and the transition to active DNA packaging. We show that ATP plays a major role in regulating all of these activities and may serve as a 'nucleotide switch' that mediates complex assembly, nuclease activation and *cos*-clearance steps. These features are recapitulated and conserved in all of the dsDNA viruses and the results described herein for λ have broad implications.

MATERIALS AND METHODS

Protein and DNA preparation

The terminase protomer was purified by published protocol (16,19). Briefly, the terminase 'mix' was purified chromatographically using a HisTrap FF column followed by a HiTrap Q column. The structurally homogenous protomer was then isolated using a HiPrep S-300 gel filtration column. The purified enzyme is >98% homogenous as determined by SDS-PAGE and the protomeric species is greater than >98% structurally homogenous as determined by sedimentation velocity analytical ultracentrifugation analysis (25). IHF was isolated as described in Sanyal *et al.* (17). Procapsids were purified as previously described using the heat-inducible MF869 lysogen (a generous gift from Michael Feiss) (32). A 274 bp duplex that contains the minimal *cos* sequence for use in the EMSA studies was prepared by large-scale preparative PCR as previously described (17).

DNA maturation assay

The *cos*-cleavage endonuclease reaction was performed as described previously with slight modification (19). Briefly, the reaction mixtures (20 μL) contained 50 mM Tris buffer, pH 8.6 at 4°C, 10 mM MgCl$_2$, 20 mM NaCl, 7 mM β-Me, 2% glycerol and 20 nM ScaI-linearized pAFP1 DNA substrate (3 kb). IHF (50 nM) and nucleotides were included as indicated in each experiment. The reactions were initiated with the addition of the terminase protomer (200 nM), allowed to proceed for 30 min at 37°C and then quenched with 15 mM EDTA. The extent of *cos*-cleavage (duplex nicking) was analyzed by heating the quenched reaction mixture to 70°C for 5 min prior to loading onto a 1% agarose gel. The 3 kb substrate and the nuclease product bands (D_L (1 kb) and D_R (2 kb)) were quantified by video densitometry and unless otherwise indicated, the kinetic data were analyzed according to the simple monophasic exponential model as described previously (19).

A

B
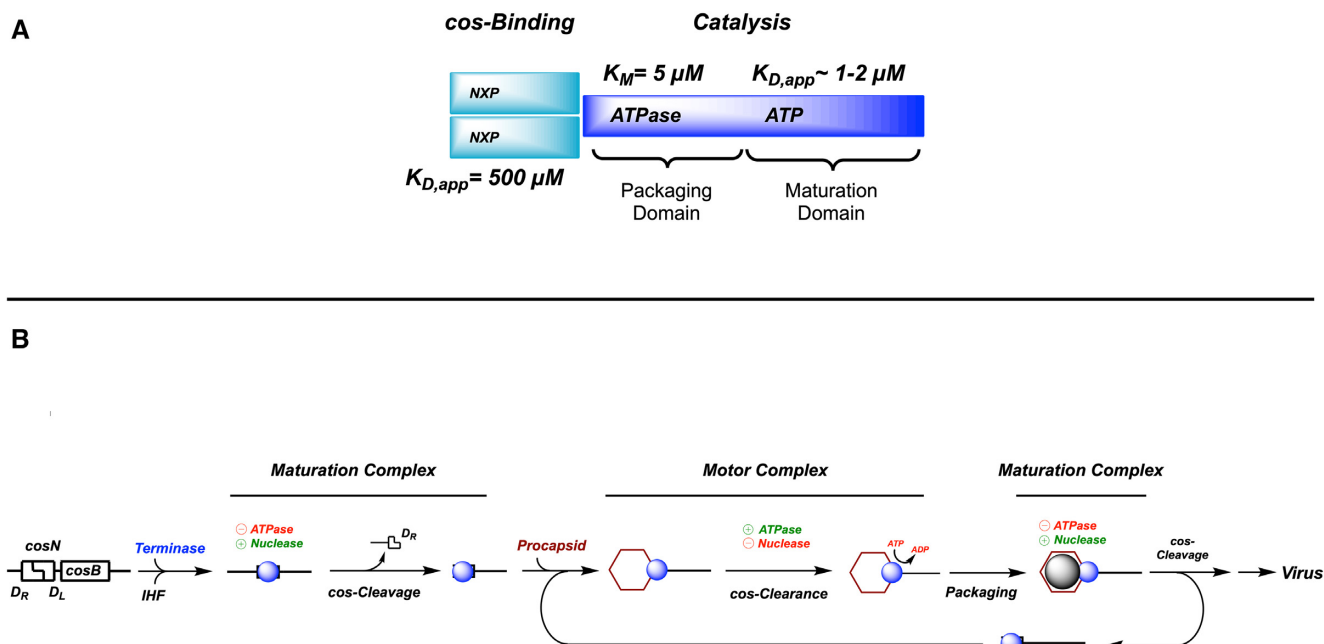
Figure 1. Lambda terminase and assembly of a virus particle. (**A**) The lambda terminase protomer is composed of one catalytic subunit (TerL) and two DNA binding subunits (TerL$_1$•TerS$_2$, blue and cyan, respectively). Three functional nucleotide binding sites have been identified in the protomer (see (23) for a detailed discussion); (i) a low-affinity site in TerS that binds ATP, ADP, GTP and GDP (NXP) and that regulates DNA binding interactions. NXP binding to this site also stimulates packaging ATPase activity in TerL; (ii) a high-affinity packaging ATPase site in the N-terminal DNA packaging domain that powers DNA translocation by the packaging motor; (iii) a high-affinity site in the C-terminal genome maturation site in TerL that binds ATP and that is the focus of the present work. (**B**) Model for genome maturation and packaging by lambda terminase. The enzyme processively excises and packages individual genomes from a concatemeric DNA precursor, alternating between a stable, site-specifically bound maturation complex and a dynamic packaging motor complex. The terminase complexes are represented as blue balls for simplicity. Biophysical data suggest that the maturation complex is composed of four protomers that encircle the duplex at the *cos*-site [(TerL$_1$•TerS$_2$)$_4$] (16). A tetrameric complex would thus contain four maturation ATP binding sites and four packaging ATPase sites in the four TerL catalytic subunits, plus eight nucleotide binding sites in the presumed octameric TerS DNA binding ring. Kinetic interrogation of the enzyme has revealed complex allosteric interactions between all of these sites (see (23)). Details are provided in the text.

DNA packaging assay

Packaging activity was quantified as previously described (15) with slight modification employing a two-step protocol to optimize each step in the packaging pathway (see Figure 3, *top*). In *step 1*, the *cos*-cleavage reaction was employed to generate the post-cleavage maturation complex as described above, except that pCT-λ, a 12.2 kb *cos*-containing packaging substrate was used; IHF (50 nM) and nucleotides were included as indicated in each individual experiment. In *step 2*, procapsids (40 nM) and ATP (2 mM) were added to initiate the packaging reaction, which was allowed to proceed for 20 minutes at 25°C. DNAse (20 µg/ml) was then added and the mixture was incubated at 25°C for 5 min to digest unpackaged DNA. The reaction was quenched with the addition of an equal volume of phenol-chloroform, which also denatures the capsid shells to release the DNase resistant (e.g. packaged) DNA, which was quantitated by agarose gel assay as previously described (15).

Electrophoretic mobility shift (EMS) studies

The binding experiments were performed as previously described using a ^{32}P-end labeled 274 bp *cos* substrate (33). Binding conditions were as follows.

DNA maturation complexes (step 1). The terminase protomer (100 nM), IHF (5 nM) and ^{32}P labeled DNA (30 pM) were mixed in binding buffer containing 20 mM Tris, pH 8.6 at 4°C, 50 mM NaCl, 10 mM MgCl, 7 mM β-Me, 100 µg/ml BSA, 2 µg/ml salmon sperm DNA and 10% glycerol; nucleotides were included as indicated in each individual experiment. The mixture was incubated at 30°C for 20 min to afford the post-cleavage maturation complex. Un-labeled *cos* 274-bp competitor DNA (10 nM) was then added prior to electrophoretic analysis.

Packaging motor complexes (step 2). Procapsids (40 nM) and ATP (2 mM) were added to the post-cleavage maturation complexes generated in *step 1* above and the samples were incubated at room temperature for 20 min to assemble the motor complexes and to initiate the packaging reaction. DNase and phenol-chloroform were then added as indicated to digest un-packaged DNA and to denature the capsid shells to release packaged DNA, respectively.

In all cases, unbound DNA and the protein-DNA complexes were fractionated on a 5% low-cross linking (1.2%) acrylamide gel and the radioactive bands were visualized and quantified as described in Ortega and Catalano (33).

RESULTS

AXP stimulates the cos-cleavage genome maturation reaction

We previously described biochemical studies on the *cos*-specific endonuclease activity of λ terminase, a.k.a., the genome maturation reaction (22,34,35). Our prior studies utilized terminase preparations that were pure, but structurally heterogeneous (the terminase mix). Since that time, we have purified the enzyme as a stable and homogenous complex composed of one TerL subunit tightly associated with two TerS subunits (the terminase protomer) (16,24,25). Here, we interrogate the catalytic requirements for *cos*-cleavage by the λ terminase protomer and further define the role of nucleotides in modulating the reaction. Within this context, we have identified three nucleotide binding sites in the protomer (see Figure 1A); (i) a low affinity site in TerS that binds both adenosine and guanosine nucleotides (NXP, $K_{D,app} \sim 500$ μM) (36), (ii) a high affinity ATP binding site in the C-terminal genome maturation domain of TerL ($K_{D,app} \sim 1$–2 μM) (18) and (iii) a high-affinity ATPase catalytic site in the N-terminal DNA packaging domain that is associated with powering DNA translocation (the packaging ATPase, $K_M \sim 5$ μM) (23,38,39). Based on these rel-

ative affinities, nucleotide interactions with the TerL subunit can be probed using low concentrations of nucleotide (50 μM) whereas binding to the TerS subunit requires elevated (mM) nucleotide concentrations. Unless otherwise indicated, all of our studies used 50 μM nucleotides which precludes binding to the TerS DNA binding subunit.

The terminase protomer possesses a weak *cos*-cleavage activity that is significantly stimulated by both ATP and ADP (herein referred to as *AXP*), while AMP has little effect (Figure 2A, B). We examined the concentration dependence of the observed stimulation by ADP and the data are well described by a simple Langmuir binding model, which affords a $K_{D,app} = 2.6 \pm 0.4$ μM (not shown). This binding constant is well below that of the NXP binding site in TerS ($K_{D,app} = 500$ μM) and implicate a high-affinity site in the TerL subunit (see Figure 1A). While we cannot rigorously exclude the packaging ATPase binding site, we find this unlikely and we interpret the data to indicate that AXP binding to the ATP binding site in the maturation domain of TerL is responsible for nuclease activation. We next examined the non-hydrolysable ATP analog β,γ-methyleneadenosine 5′-triphosphate (AMP-PCP) for its capacity to stimulate *cos*-cleavage activity. Figure 2B shows
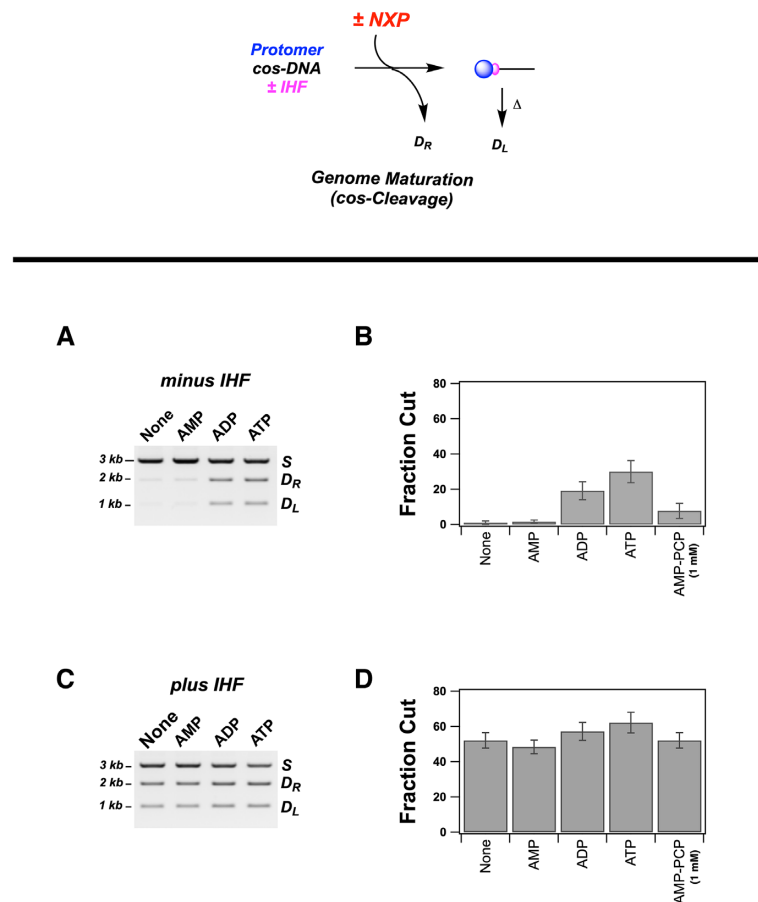
Figure 2. AXP stimulates the *cos*-cleavage reaction. (**A**) Agarose gel showing the products of *cos*-cleavage. The reaction was performed as described in Materials and Methods in the absence of IHF but in the presence of the indicated nucleotide (50 μM). Specific cleavage at the *cos*-sequence in the 3 kb DNA substrate (*S*) affords 1 kb and 2 kb products (D_L, D_R, respectively). (**B**) Quantitation of the data presented in (A) plus that for a *cos*-cleavage reaction containing 1 mM AMP-PCP. (**C**) The *cos*-cleavage reaction was performed in the presence of IHF and the indicated nucleotide (50 μM). (**D**) Quantitation of the data presented in *Panel C* plus that for a *cos*-cleavage reaction containing 1 mM AMP-PCP.

that the nucleotide analog only partially stimulates the reaction even at a concentration of 1 mM. To confirm that AMP-PCP binds to the enzyme at this concentration, we examined the concentration dependence and the observed stimulation are well described by a simple Langmuir binding model, which affords a $K_{D,app} = 54 \pm 10$ μM (not shown). While elevated relative to ADP, this binding constant is similarly well below that of the NXP binding site in TerS implicate the high-affinity maturation site in TerL.

Role of IHF in the cos-Cleavage reaction

The *Escherichia coli* integration host factor (IHF) is required for efficient λ development *in vivo* (41). We previously demonstrated that (i) the terminase protomer alone binds DNA weakly ($K_{D,app} \sim 150$ nM), (ii) that IHF and terminase cooperatively bind to *cos*-DNA with high specificity and affinity ($K_{D,app} \sim 20$ nM) and (iii) that the assembled maturation complex efficiently cuts the duplex at *cos* in the presence of Mg^{2+} (26). The data presented in Figure 2C and D recapitulate these results using the terminase protomer and further demonstrate that nucleotides little affect the reaction in the presence of IHF, i.e. additivity is not observed.

AXP is required for the transition to packaging

Subsequent to duplex nicking the stable, site-specifically bound maturation complex binds to the portal of an empty procapsid to assemble the motor complex. The activated motor then releases the matured genome end (D_L) and initiates the DNA packaging reaction (*cos*-clearance, Figure 1B). We here probe the nucleotide requirement for the transition to packaging using a two-step protocol, as outlined in Figure 3. In *step 1*, the *cos*-cleavage reaction is initiated by mixing the terminase protomer and *cos*-DNA, plus or minus IHF and AXP (50 μM); the reaction is allowed to proceed for 30 minutes at 37°C to afford the post-cleavage maturation complex. To initiate packaging in *step 2*, procapsids and ATP (2 mM) are added and the reaction is allowed to proceed for 20 minutes at room temperature. Packaged DNA is then quantified by DNase resistance as described in Materials and Methods. We note that *cos*-cleavage is inefficient when the reaction is conducted at 25°C (not shown). Consequently, DNA packaging in *step 2* (performed at 25°C) is dependent upon the amount of maturation complex assembled in *step 1* of the reaction (performed at 37°C).

Consistent with the observation that AXP stimulates the *cos*-cleavage reaction (Figure 2B), the data presented in Figure 3A demonstrate that both ATP and ADP stimulate DNA packaging *when included in step 1 of the reaction*, i.e., during maturation complex assembly. Of note, selective packaging of the matured D_L end is observed under these conditions. In contrast, while IHF also stimulates the *cos*-cleavage reaction (Figure 2D), the host protein alone does *not* support the transition to packaging (Figure 3B). When AXP and IHF are both included in ***step 1***, additivity is observed and the host protein stimulates AXP-promoted packaging 2–3-fold (compare Figure 3A, B). Importantly, *both must be present during maturation complex assembly*

(*step 1*) as addition of IHF or ADP in *step 2* has no effect on packaging (data not shown). Similar to the *cos*-cleavage reaction, AMP-PCP (1 mM) partially stimulates the reaction while AMP has little effect (Figure 3C).

To further probe the *cos*-clearance transition, we varied the ADP concentration in *step 1* and determined the extent of DNA packaging upon addition of procapsids and ATP in *step 2*. The data presented in Figure 3D reveal a hyperbolic activation curve and quantification of the data according to a Langmuir model affords a $K_{D,app} = 18 \pm 4$ μM. As with *cos*-cleavage, these data implicate the high-affinity maturation site in TerL.

AXP is required for maturation complex stability

The data above demonstrate that ATP or ADP must be present during maturation complex assembly (*step 1*) to ensure efficient transition to DNA packaging (*step 2*). This observation suggests that nucleotides are required for efficient procapsid binding and/or for subsequent 'cos-clearance' steps. We first considered that AXP might be required to stabilize the post-cleavage maturation complex such that it can productively bind the procapsid using an electrophoretic mobility shift (EMS) approach.

The maturation complex was assembled with protomer, IHF, *cos*-DNA and the indicated nucleotide as outlined Figure 3 (*step 1, top*). In the absence of nucleotide, the EMS data reveal (i) two strongly retarded bands that we attribute to terminase–DNA complexes (C1 and C2), (ii) the upstream D_R fragment generated in the *cos*-cleavage reaction that has been ejected from the complexes and (iii) a small amount of free D_L fragment (Figure 4A). In addition, a significant band co-migrating with the substrate (S) is observed. Heating the binding mixture quantitatively affords D_R and D_L fragments (lane Δ), which indicates that this band represents the nicked, annealed duplex product of the *cos*-cleavage reaction that has dissociated from the enzyme (S_{nicked}). An identical pattern is observed in the presence of 50 μM AMP (Figure 4) and 1 mM AMP-PCP (data not show); however, addition of ATP or ADP to the binding mixture results in an increase in the intensity of the D_R band, disappearance of the S_{nicked} band and a concomitant increase in the fraction of the C2 complex at the expense of C1. Once assembled the AXP-complex is stable for at least 3 h at room temperature (data not shown).

To further explore the role of nucleotide on maturation complex assembly, we examined the ADP concentration dependence. The data presented in Figure 4B and C show that as the ADP concentration is increased, there is a concomitant increase in the C2 complex at the expense of C1, disappearance of the S_{nicked} band and an increase in the intensity of the free D_R band. The concentration dependence ($K_{D,app} \sim 10$ μM) suggests that ADP binding to the maturation domain in TerL is required for this transition. We interpret the ensemble of data to indicate that the C1 band represents terminase bound to the nicked, annealed duplex (S_{nicked}) and that the C2 band represents terminase bound to the D_L fragment that is to be packaged and from which the unpackaged D_R fragment has been ejected. The data further reveal that AXP binding to the maturation site in TerL
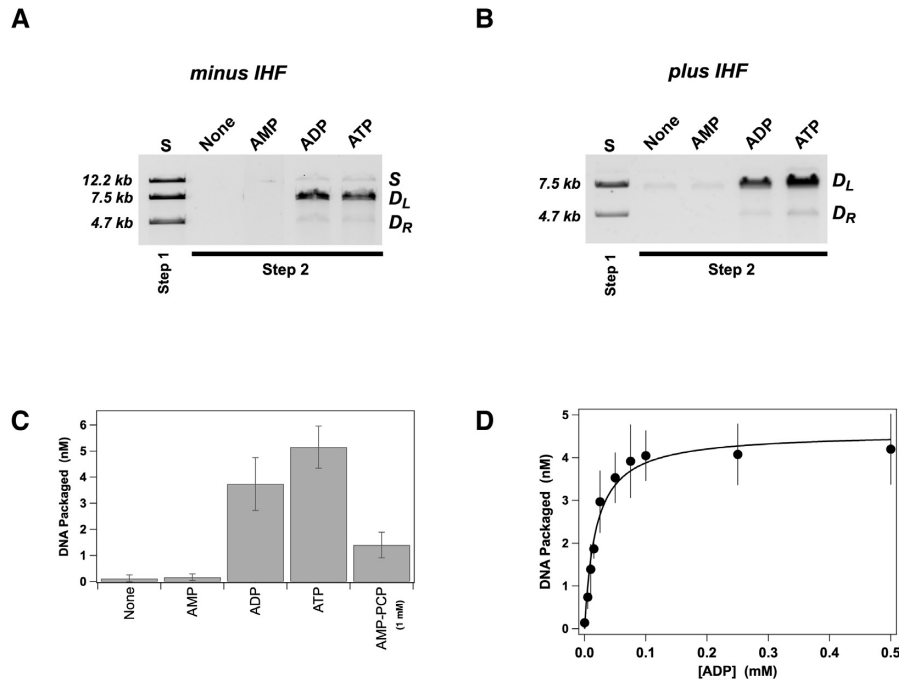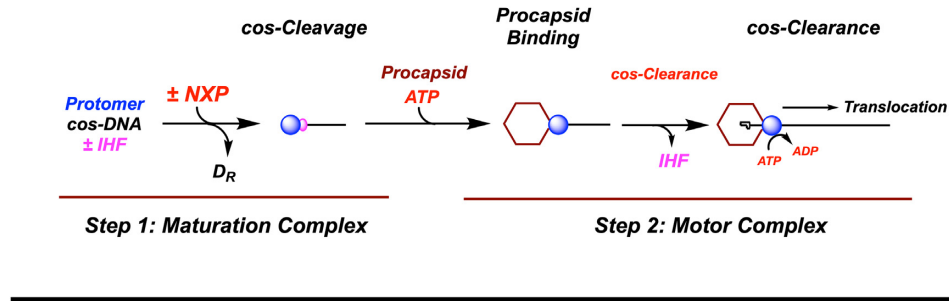
Figure 3. AXP is required for the transition to DNA packaging. The DNA packaging reaction was performed in two steps as described in Materials and Methods and as outlined at top of the figure. (**A**) The *cos*-cleavage reaction (*step 1*) was performed in the absence of IHF but in the presence of the indicated nucleotide (50 μM). The first lane shows the products of the *cos*-cleavage reaction with the migration of un-cut substrate (**S**, 12.2 kb) and the two nuclease products ($D_L \sim$ 7.5 kb, $D_R \sim$ 4.7 kb) indicated. This was the input DNA for the packaging reaction (*step 2*) and DNase resistant (packaged) DNA is shown in the gel. Note that only the D_L strand is packaged. (**B**) Same as *Panel A* except that IHF was included in *step 1* of the reaction. The substrate was totally cut under these conditions (lane S). This was the input DNA for the packaging reaction (*step 2*) and DNase resistant (packaged) DNA is shown in the agarose gel. (**C**) Quantitation of the data presented in Panel B plus that for a packaging reaction containing 1 mM AMP-PCP *in step 1*. (**D**) The *cos*-cleavage reaction (*step 1*) was performed in the presence of IHF and in the presence of varying concentrations of ADP, as indicated, followed by DNA packaging (*step 2*). Each data point represents the average of three separate experiments with standard deviation shown in bars. The solid line represents the best fit of the data to a Langmuir binding model.

is required for efficient ejection of the D_R fragment and for stabilization of the terminase–DNA complexes.

Procapsid capture and cos-clearance

Once generated, the post-cleavage maturation complex binds to the portal vertex of a procapsid to afford the packaging motor (Figure 1B). To interrogate this step in the packaging pathway, we assembled the maturation complex in the presence of ADP to afford the C2 complex, as described above. Addition of procapsids results in the disappearance of the C2 band, the appearance of a strongly retarded band, but little effect on the free D_R band (Figure 5). We ascribe the strongly retarded band to the ter-

minase motor complex assembled to the portal vertex of a procapsid. Subsequent addition of ATP, to power DNA packaging, does not significantly affect the pattern. Addition of DNase degrades the free D_R fragment but does not affect DNA incorporated into the packaging motor complex. Phenol-chloroform extraction of the DNase-treated mixture degrades the capsid and releases the intact D_L fragment, indicating that it has been packaged into the procapsid shell (Figure 5).

DISCUSSION

Double-stranded DNA viruses that replicate their DNA as multi-genome concatemers, both prokaryotic and eukary-
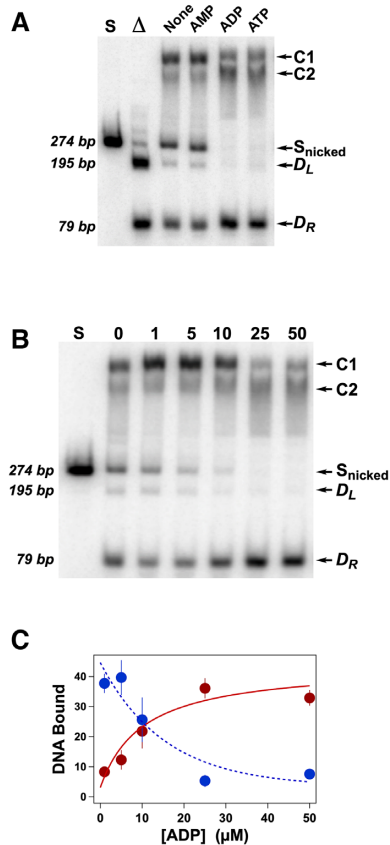
Figure 4. AXP stabilizes post-nicking maturation complex. (**A**) The *cos*-cleavage reaction was performed in the presence of IHF and the indicated nucleotide (50 µM) as described in Materials and Methods. The gel shows an electrophoretic mobility gel shift assay (EMSA) of the reaction products. *Lane S*, the *cos*-containing ^{32}P-labeled 274 bp duplex substrate. Δ, a representative reaction mixture heated to 70°C for 5 min to dissociate the nicked, annealed duplex generated in the *cos*-cleavage reaction. Note that in the absence of IHF, terminase binds DNA weakly and non-specifically, and neither the C1 nor C2 bands are observed (26). (**B**) The *cos*-cleavage assay was performed as in Panel A in the presence of ADP in *step 1* at the indicated concentration. *Lane S,* the *cos*-containing ^{32}P-labeled 274 bp duplex substrate. (**C**) Quantitation of the data presented in Panel B showing the transition from C1 (blue) to C2 (red) complexes. Each data point represents the average of three separated experiments with standard deviation indicated in bars. The solid red line represents the best fit of the C2 data to a Langmuir binding model ($K_{D,app} \sim 10$ µM); the dashed blue line is presented to guide the eye.

otic, all encode a terminase enzyme that processively excises and packages monomeric genomes. These coordinated reactions and the protein complexes that catalyze them are strongly conserved but remain ill studied and poorly understood. Processive packaging requires that the enzymes alternate between a stable nuclease complex and dynamic motor complex, respectively. The biochemical features regulating these cyclic transitions remain obscure, but the studies presented herein provide mechanistic insight into these conserved reactions. The data reveal that ATP plays a central role in both maturation complex assembly and activation, and in the transition to packaging. The data further suggest that these events are regulated by AXP occupancy of the high-affinity binding site in the maturation domain of TerL (Figure 1A). That AMP-PCP partially supports
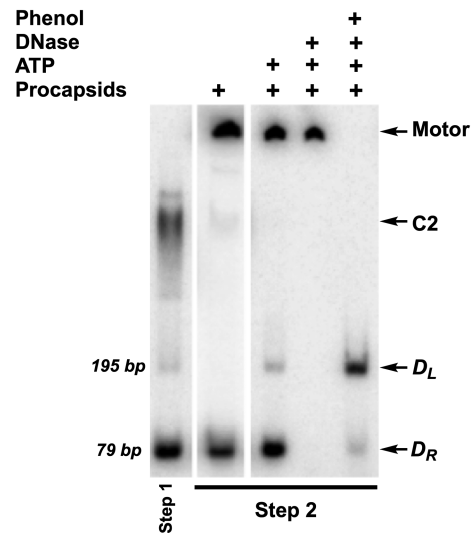
Figure 5. Procapsid capture and *cos*-clearance. The post-cleavage maturation complex was assembled as described in Materials and Methods with IHF and ADP (50 µM) included in the reaction mixture (*lane 1*). Procapsids and ATP were then added, as indicated, to generate the packaging motor complex assembled on the procapsid, followed by DNase digestion and phenol extraction, as indicated.

these reactions indicates that ATP may play a role; however, the maturation site hydrolyzes ATP in a single catalytic turnover indicating that ADP release is slow and that the dinucleotide remains stably bound at the allosteric site once hydrolyzed (37). Scheme 1 provides a unified model for maturation complex assembly, nuclease activation and the transition to packaging that encompasses both published data and that presented here.

Maturation complex assembly and nuclease activation

The resting terminase protomer binds DNA weakly and non-specifically and thus possesses little to no *cos*-cleavage activity. We propose that AXP bound at the maturation site of TerL drives an enzyme conformation that can recognize the *cos*-sequence in the absence of IHF; however, this intermediate is thermodynamically unstable and nuclease activity is weak. Efficient assembly of the maturation complex and nuclease activation requires IHF (Figure 2). In all known cases, the host protein binds to cognate recognition sites in DNA and introduces a strong bend in the duplex which provides an architecture conducive to assembly of additional proteins at that site (41,42). Indeed, we have demonstrated that IHF and terminase cooperatively bind and bend *cos*-containing DNA duplexes (>160°) to afford a catalytically-competent nuclease complex in the absence of nucleotides (16,33). Given that the concentration of terminase is ~100 nM in an infected cell and that IHF is always present, the dark arrows in Scheme 1 represent the biological relevant pathway *in vivo*.

Transition to packaging

Once generated, the post-cleavage maturation complex binds to the portal of a pre-assembled procapsid to afford
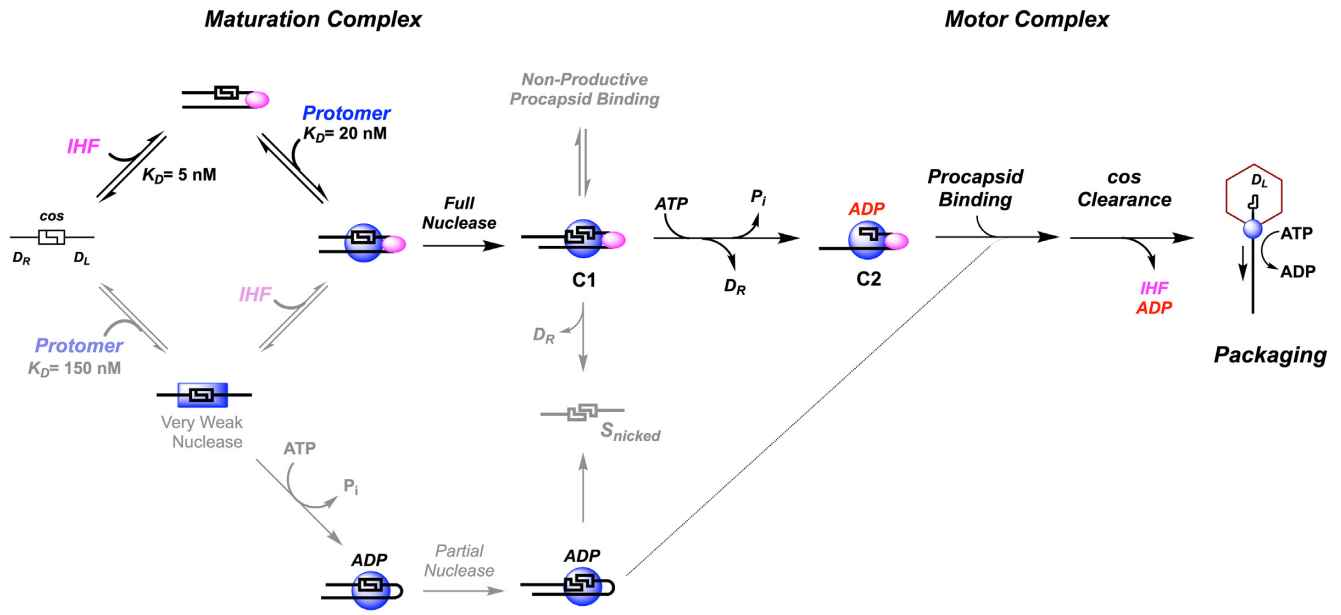
Scheme 1. Model for coordinated maturation and packaging motor complex assembly and function. Light arrows and complexes represent biochemically characterized but off-pathway reactions characterized *in vitro*. Dark arrows represent complexes biochemically characterized *in vitro*, and the preferred pathway during a productive infection *in vivo*. Details are presented in the text.

the activated packaging motor, which triggers *cos*-clearance and the transition to packaging. The kinetic data reveal an intricate interplay between IHF and ATP in the transition to packing, as follows. The nuclease activity of terminase is maximally stimulated by IHF alone and this intermediate can bind procapsids; however, the resulting motor is incompetent for the transition to packaging (Figure 3B). In contrast, while AXP alone can partially stimulate the maturation reaction and despite the fact that this complex is unstable, it can bind to the procapsid and weakly packaging the matured D_L strand (Figure 3A). Robust packaging requires that *both* IHF and AXP are present during maturation complex assembly. We interpret the ensemble of data as follows.

In the absence of ATP, terminase and IHF assemble at *cos* and nick the duplex to afford a protein complex bound to the nicked, annealed DNA substrate (C1, Scheme 1). This intermediate is unstable and a significant fraction of S_{nicked} dissociates from the enzyme. Further, while the C1 complex can bind to a procapsid, it does so in an unproductive fashion and the transition to packaging is severely compromised. AXP bound at the maturation binding site is required for efficient ejection of D_R to afford the C2 complex and productive binding to the procapsid, as depicted in Scheme 1. *In vivo*, this is mediated by ADP as a result of ATP binding and single-turnover hydrolysis at that site (*vide supra*). We presume that procapsid binding triggers IHF release from the DNA and ADP dissociation from the enzyme, both of which allow resolution of the bent duplex architecture, *cos*-clearance and the transition to packaging. In this manner, ATP may serve as a 'nucleotide switch' that coordinates the activity of two distinct catalytic complexes essential to processive genome packaging.

In addition to the role of ATP in nuclease activation and *cos* clearance, it is important to note that the packaging

ATPase site must also be activated in the transition to packaging. Prior studies in our lab suggest that the low affinity nucleotide binding site in TerS subunit (Figure 1B) plays an important role in this regard. This site binds both adenosine and guanosine di- and tri-nucleotides (NXP), which stimulates both ATP hydrolysis by the packaging ATPase site in TerL (23,36) and DNA packaging (Yang and Catalano, unpublished). Thus, ATP serves as a master allosteric regulator, integrating signals from (i) the AXP binding site in TerL, which stabilizes the maturation complex and is essential for the transition to packaging, and from (ii) the NXP binding site in TerS that regulates packaging ATPase and motor activity. These intricate interactions likely play a central role in the cyclic interconversion of the maturation vs. motor complexes during processive genome packaging, particularly by the unit-length genome packaging viruses such as λ and the herpesviruses, among others (1–3). In these viruses, the translocating motor is captured by a downstream *cos* site (or 'a' site in the herpesviruses) which triggers a transition back to a stable maturation complex bound at the genome end. The TerS subunits are responsible for recognition of the *cos* sequence and must play an active role in the cyclic transitions required for processive packaging.

In contrast, while 'headful' phages, such as SPP1 and P74-26 initiate packaging at a specific '*pac*' site in the concatemer, the motors bypass the downstream *pac* site and continue packaging until a head full DNA length has been inserted into the shell. This results in virions that contain DNA 104%-110% larger than the unit-length genomes (3,43). While these phages require a TerS subunit to initiate packaging from a genome concatemer, subsequent cuts are made in a non-specific manner and the TerS subunits are not strictly required. In these cases, processive packaging may be mediated by the TerL subunits alone, though

cyclic regulation of both nuclease and packaging ATPase catalytic activities remains necessary. Within this context, we note that ATP stimulates the nuclease activity of TerL subunits in the P22 (44), Sf6 (45) and P74-26 (46) phage systems, but this has not been studied in detail. Further, a second ATP binding site, distinct from the packaging ATPase site was also proposed in the maturation domain of the phage T4 TerL subunit based on sequence homology (47); however, genetic studies did not reveal a defined function for the putative site (48). It is feasible that this cryptic site plays a similar role in processive genome packaging and that the nucleotide switch mechanism identified here may play a role in all dsDNA viruses that package concatemeric DNA.

CONCLUSIONS

The present study reveals a complex regulatory circuit modulated by IHF (at the level of DNA) and ATP (at the level of the enzyme) in the assembly of the genome maturation complex, activation of maturation nuclease activity and subsequent assembly of a catalytically competent motor complex. These biological processes are recapitulated in all of the dsDNA viruses that package monomeric genomes from concatemeric DNA substrates, from phages to herpesviruses. Thus, a nucleotide switch mechanism for regulated progression through the packaging intermediates identified here has broad biological implications with respect to general virus assembly mechanisms. Finally, we note that ATP plays analogous mechanistic roles in the site-specific assembly of DNA replication complexes and their transition to dynamic synthetic motor complexes (49,50) further broadening the biological implications of the present study.

FUNDING

REFERENCES

1. Knipe,D.M. and Howley,P.M. (2007) In: *Fields Virology*. 5th edn. Lippincott-Williams, and Wilkins, NY.
2. Calendar,R. and Abedon,S.T. (2006) In: *The Bacteriophages*. Oxford University Press, NY.
3. Catalano,C.E. (2005) In: Catalano,CE (ed). *Viral Genome Packaging Machines: Genetics, Structure, and Mechanism*. Kluwer Academic/Plenum Publishers, NY, pp. 1–4.
4. Ahi,Y.S. and Mittal,S.K. (2016) Components of adenovirus genome packaging. *Front. Microbiol.*, **7**, 1503.
5. Häuser,R., Blasche,S., Dokland,T., Haggård-Ljungquist,E., von Brunn,A., Salas,M., Casjens,S., Molineux,I. and Uetz,P. (2012) In: Małgorzata,Ł and Wacław,S (eds). *Advances in Virus Research*. Academic Press, Vol. **83**, pp. 219–298.
6. Baines,J.D. (2011) Herpes simplex virus capsid assembly and DNA packaging: a present and future antiviral drug target. *Trends Microbiol.*, **19**, 606–613.
7. Black,L.W. (2015) Old, new, and widely true: The bacteriophage T4 DNA packaging mechanism. *Virology*, **479–480**, 650–656.
8. Casjens,S.R. (2011) The DNA-packaging nanomotor of tailed bacteriophages. *Nat. Rev. Micro*, **9**, 647–657.
9. Anderson,D. and Grimes,S. (2005) In: Catalano,CE (ed). *Viral Genome Packaging Machines: Genetics, Structure, and Mechanism*. Kluwer Academic/Plenum Publishers, NY, pp. 103–116.
10. Baines,J.D. and Weller,S.K. (2005) In: Catalano,CE (ed). *Viral Genome Packaging Machines: Genetics, Structure, and Mechanism*. Kluwer Academic/Plenum Publishers, NY, pp. 135–149.
11. Feiss,M. and Rao,B.N. (2012) In: Rossmann,MG and Rao,BN (eds). *Viral Molecular Machines*. Springer US, pp. 498–509.
12. Feiss,M. and Catalano,C.E. (2005) In: Catalano,CE (ed). *Viral Genome Packaging Machines: Genetics, Structure, and Mechanism*. Kluwer Academic/Plenum Publishers, NY, pp. 5–39.
13. Jardine,P.J. and Anderson,D.L. (2006) In: Calendar,R and Abedon,ST (eds). *The Bacteriophages*. 2nd edn. Oxford University Press, NY, pp. 49–65.
14. Gaussier,H., Yang,Q. and Catalano,C.E. (2006) Building a virus from scratch: assembly of an infectious virus using purified components in a rigorously defined biochemical assay system. *J. Mol. Biol.*, **357**, 1154–1166.
15. Andrews,B.T. and Catalano,C.E. (2013) Strong Subunit Coordination Drives a Powerful Viral DNA Packaging Motor. *Proc. Natl. Acad. Sci. U.S.A.*, **110**, 5909–5914.
16. Yang,T.-C., Ortiz,D., Nosaka,L.A., Lander,G.C. and Catalano,C.E. (2015) Thermodynamic interrogation of the assembly of a viral genome packaging motor complex. *Biophys. J.*, **109**, 1663–1675.
17. Sanyal,S.J., Yang,T.-C. and Catalano,C.E. (2014) Integration host factor assembly at the cohesive end site of the bacteriophage lambda genome: Implications for viral DNA packaging and bacterial gene regulation. *Biochemistry*, **53**, 7459–7470.
18. Chang,J.R., Andrews,B.T. and Catalano,C.E. (2012) Energy-independent helicase activity of a viral genome packaging motor. *Biochemistry*, **51**, 391–400.
19. Andrews,B.T. and Catalano,C.E. (2012) The enzymology of a viral genome packaging motor is influenced by the assembly state of the motor subunits. *Biochemistry*, **51**, 9342–9353.
20. Yang,Q., Catalano,C.E. and Maluf,N.K. (2009) Kinetic analysis of the genome packaging reaction in bacteriophage lambda. *Biochemistry*, **48**, 10705–10715.
21. Yang,Q., Maluf,N.K. and Catalano,C.E. (2008) Packaging of a Unit-length viral genome: The role of nucleotides and the gpD decoration protein in stable nucleocapsid assembly in bacteriophage lambda. *J. Mol. Biol.*, **383**, 1037–1048.
22. Yang,Q. and Catalano,C.E. (2004) A minimal kinetic model for a viral DNA packaging machine. *Biochemistry*, **43**, 289–299.
23. Catalano,C.E. (2019) In: *Reference Module in Life Sciences*. Elsevier, pp. 1–13.
24. Maluf,N.K., Gaussier,H., Bogner,E., Feiss,M. and Catalano,C.E. (2006) Assembly of bacteriophage lambda terminase into a viral DNA maturation and packaging machine. *Biochemistry*, **45**, 15259–15268.
25. Maluf,N.K., Yang,Q. and Catalano,C.E. (2005) Self-association properties of the bacteriophage lambda terminase holoenzyme: implications for the DNA packaging motor. *J. Mol. Biol.*, **347**, 523–542.
26. Yang,T.-C., Ortiz,D., Yang,Q., Angelis,R.D., Sanyal,S.J. and Catalano,C.E. (2017) Physical and functional characterization of nucleoprotein complexes along a viral assembly pathway. *Biophys. J.*, **112**, 1551–1560.
27. Yang,Q., Hanagan,A. and Catalano,C.E. (1997) Assembly of a nucleoprotein complex required for DNA packaging by bacteriophage lambda. *Biochemistry*, **36**, 2744–2752.
28. Hohn,T., Wurtz,M. and Hohn,B. (1976) Capsid transformation during packaging of bacteriophage lambda DNA. *Phil. Trans. R. Soc. Lond.*, **276**, 51–61.
29. Dokland,T. and Murialdo,H. (1993) Structural transitions during maturation of bacteriophage lambda capsids. *J. Mol. Biol.*, **233**, 682–694.
30. Hendrix,R.W. and Casjens,S. (2006) In: Calendar,R and Abedon,ST (eds). *The Bacteriophages*. 2nd edn. Oxford University Press, NY, pp. 409–447.
31. Medina,E., Nakatani,E., Kruse,S. and Catalano,C.E. (2012) Thermodynamic characterization of viral procapsid expansion into a functional capsid shell. *J. Mol. Biol.*, **418**, 167–180.
32. Yang,Q. and Catalano,C.E. (2003) Biochemical characterization of bacteriophage lambda genome packaging in vitro. *Virology*, **305**, 276–287.
33. Ortega,M.E. and Catalano,C.E. (2006) Bacteriophage lambda gpNu1 and Escherichia coli IHF proteins cooperatively bind and bend viral

DNA: implications for the assembly of a genome-packaging motor. *Biochemistry*, **45**, 5180–5189.

34. Woods,L., Terpening,C. and Catalano,C.E. (1997) Kinetic analysis of the endonuclease activity of phage lambda terminase: assembly of a catalytically competent nicking complex is rate-limiting. *Biochemistry*, **36**, 5777–5785.

35. Tomka,M.A. and Catalano,C.E. (1993) Physical and kinetic characterization of the DNA packaging enzyme from bacteriophage lambda. *J. Biol. Chem.*, **268**, 3056–3065.

36. Woods,L. and Catalano,C.E. (1999) Kinetic characterization of the GTPase activity of phage lambda terminase: evidence for communication between the two 'NTPase' catalytic sites of the enzyme. *Biochemistry*, **38**, 14624–14630.

37. Ortega,M.E., Gaussier,H. and Catalano,C.E. (2007) The DNA maturation domain of gpA, the DNA packaging motor protein of bacteriophage lambda, contains an ATPase site associated with endonuclease activity. *J. Mol. Biol.*, **373**, 851–865.

38. Tomka,M.A. and Catalano,C.E. (1993) Kinetic characterization of the ATPase activity of the DNA packaging enzyme from bacteriophage lambda. *Biochemistry*, **32**, 11992–11997.

39. Ortiz,D., delToro,D., Ordyan,M., Pajak,J., Sippy,J., Catala,A., Oh,C.-S., Vu,A., Arya,G., Feiss,M *et al.* (2019) Evidence that a catalytic glutamate and an 'Arginine Toggle' act in concert to mediate ATP hydrolysis and mechanochemical coupling in a viral DNA packaging motor. *Nucleic Acids Res.*, **47**, 1404–1415.

40. Hwang,Y., Catalano,C.E. and Feiss,M. (1996) Kinetic and mutational dissection of the two ATPase activities of terminase, the DNA packaging enzyme of bacteriophage Chi. *Biochemistry*, **35**, 2796–2803.

41. Mendelson,I., Gottesman,M. and Oppenheim,A.B. (1991) HU and integration host factor function as auxiliary proteins in cleavage of phage lambda cohesive ends by terminase. *J. Bacteriol.*, **173**, 1670–1676.

42. Swinger,K.K. and Rice,P.A. (2004) IHF and HU: flexible architects of bent DNA. *Curr. Opin. Struct. Biol.*, **14**, 28–35.

43. Rao,V.B. and Feiss,M. (2015) Mechanisms of DNA packaging by large double-stranded DNA viruses. *Annu. Rev. Virol.*, **2**, 351–378.

44. Roy,A. and Cingolani,G. (2012) Structure of P22 headful packaging nuclease. *J. Biol. Chem.*, **287**, 28196–28205.

45. Zhao,H., Christensen,T.E., Kamau,Y.N. and Tang,L. (2013) Structures of the phage Sf6 large terminase provide new insights into DNA translocation and cleavage. *PNAS*, **110**, 8075–8080.

46. Hilbert,B.J., Hayes,J.A., Stone,N.P., Xu,R.-G. and Kelch,B.A. (2017) The large terminase DNA packaging motor grips DNA with its ATPase domain for cleavage by the flexible nuclease domain. *Nucleic Acids Res.*, **45**, 3591–3605.

47. Guo,P., Peterson,C. and Anderson,D. (1987) Prohead and DNA-gp3-dependent ATPase activity of the DNA packaging protein gp16 of bacteriophage φ29. *J. Mol. Biol.*, **197**, 229–236.

48. Rao,V.B. and Mitchell,M.S. (2001) The N-terminal ATPase site in the large terminase protein gp17 is critically required for DNA packaging in bacteriophage T4. *J. Mol. Biol.*, **314**, 401–411.

49. Duderstadt,K.E. and Berger,J.M. (2013) A structural framework for replication origin opening by AAA+ initiation factors. *Curr. Opin. Struct. Biol.*, **23**, 144–153.

50. Zakrzewska-Czerwińska,J., Jakimowicz,D., Zawilak-Pawlik,A. and Messer,W. (2007) Regulation of the initiation of chromosomal replication in bacteria. *FEMS Microbiol. Rev.*, **31**, 378–387.